Pergamon

Int. J. Solids Structures Vol. 35, No. 19, pp. 2385–2406, 1998

0020-7683/98 $19.00 + .00

PII: S0020-7683(97)00142-X

MORPHOLOGY AND EFFECTIVE PROPERTIES OF DISORDERED HETEROGENEOUS MEDIA

S. TORQUATO
Department of Civil Engineering and Operations Research and Princeton Materials Institute, Princeton University, Princeton, NJ 08544, U.S.A.

(*Received* 19 *May* 1997)

Abstract—Recent progress that we have made on the problem of determining the effective properties of random heterogeneous media from knowledge of the morphology is reviewed and extended. A variety of different effective properties are considered, including the elastic moduli and electrical conductivity of composites, time scales associated with diffusion and reaction among traps, and fluid permeability of porous media. We also remark on the importance of microstructure fluctuations in influencing the failure characteristics of composites. The preponderance of work thus far has focused on heterogeneous media that are statistically homogeneous. We propose a model for statistically inhomogeneous two-phase random media (including functionally graded materials) consisting of inhomogeneous fully penetrable spheres that permits one to represent and evaluate certain n-point correlation functions that statistically characterize the microstructure for this model. Unlike the case of statistically homogeneous media, the microstructure functions depend upon the absolute positions of their arguments. Finally, we describe a novel procedure to reconstruct heterogeneous media from limited knowledge about the microstructure and discuss applications of this technique.

1. INTRODUCTION

In light of the manifest technological importance of determining the effective parameters of disordered heterogeneous materials (e.g. composite and porous media), an enormous body of literature has evolved based upon direct measurement, empirical relations, and approximate as well as rigorous theoretical methods [see Beran (1968); Bear (1972); Christensen (1979); Willis (1981); Milton and Phan-Thien (1982); Hashin (1983); Torquato (1991); Ostoja-Starzewski (1994); Torquato (1997) and references therein]. Performing direct measurements on each material sample, for all possible phase property values and volume fractions, is prohibitive from a time and cost standpoint. Empirical relations are more useful for correlating data rather than predicting them. Since bulk properties are sensitive to the details of the microstructure, a broader approach is to calculate the properties from the microscopic structure (microstructure) of the disordered material; one can then relate changes in the microstructure quantitatively to changes in the macroscopic parameters.

The random heterogeneous material is a domain of space $\mathcal{V}(\omega) \in R^d$ (where the realization ω is taken from some probability space Ω) of volume V which is composed of two regions: a phase 1 region $\mathcal{V}_1(\omega)$ of volume fraction ϕ_1 and a phase 2 region $\mathcal{V}_2(\omega)$ of volume fraction ϕ_2. Let V_i be the volume of region $\mathcal{V}_i$, $V = V_1 + V_2$ be the total system volume, $\partial\mathcal{V}(\omega)$ be the surface between $\mathcal{V}_1$ and $\mathcal{V}_2$, and S be the total surface area of the interface $\partial\mathcal{V}$. The characteristic function of phase i is defined by

$$I(\mathbf{r}, \omega) = \begin{cases} 1, & \mathbf{r} \in \mathcal{V}_i(\omega) \\ 0, & \mathbf{r} \in \mathcal{V}_2(\omega) \end{cases}. \tag{1}$$

The characteristic function of the two-phase interface is defined by

$$M(\mathbf{r}, \omega) = |\nabla I(\mathbf{r}, \omega)|. \tag{2}$$

If the media are statistically homogeneous, then *ergodicity* enables us to equate ensemble averages (indicated with angular brackets) with volume averages, i.e. averaging (1) and (2) yield

$$\phi_i = \langle I \rangle = \lim_{V_i, V \to \infty} \frac{V_i}{V}, \tag{3}$$

$$s = \langle M \rangle = \lim_{S, V \to \infty} \frac{S}{V}, \tag{4}$$

which are the porosity and specific surface (interface area per unit system volume V), respectively. Depending upon the physical context phase i can be either solid, fluid, or void. However, if the system is *statistically inhomogeneous*, then ϕ_i and s are no longer constants, but depend on the local position $\mathbf{r}$ in the heterogeneous material.

For general random media, the complexity of the microstructure prevents one from obtaining the effective properties of the system exactly. Therefore, any rigorous statement about the properties must be in the form of an inequality, i.e. rigorous bounds on the effective properties. In as far as property are concerned, this article will primarily deal with rigorous property bounds. Bounds are useful since they: (i) enable one to test the merits of theories and computer experiments; (ii) as successfully more microstructural information is incorporated, the bounds become progressively narrower; and (iii) one of the bounds can typically provide a good estimate of the property for a wide range of conditions, even when the reciprocal bound diverges from it (Torquato, 1991). Traditionally, minimum energy principles are used to generate bounds on effective properties that are expressible in terms of certain n-point correlation functions that statistically characterize the morphology. More recently, *cross-property* bounds have proven to be fruitful as well. By cross-property bounds we mean bounds on one effective property (e.g. elastic moduli) that are given in terms of other measurable properties of the same heterogeneous material (e.g. thermal or electrical conductivity).

Much of the work on bounds has been carried out for statistically homogeneous media. This will be reviewed briefly in Section 2. Here we also discuss the importance of microstructure fluctuations in determining failure characteristics of composites. In Section 3 we will describe some very recent work on a model of statistically inhomogeneous media and remark on bounds on properties for such media. Finally, in Section 4, we will report on a new procedure to reconstruct the structure of a many-particle system using limited statistical microstructural information on the system and discuss some interesting applications of this technique.

2. STRUCTURE AND PROPERTIES OF STATISTICALLY HOMOGENEOUS MEDIA

Much progress has been made in recent years in characterizing the microstructure of statistically homogeneous two-phase random media via a variety of n-point correlation functions (Torquato, 1986b, 1991). For ergodic ensembles, the n-point correlation functions are translationally invariant, that is, statistical homogeneity is implied and, hence, one can equate ensemble averages with volume averages in the infinite-volume limit. This microstructural information is fundamental in rigorously determining the effective transport, electromagnetic and mechanical properties of ergodic two-phase random media (Beran and Molyneux, 1966; Willis, 1981; Milton and Phan-Thien, 1982; Torquato, 1991, 1997).

2.1. *Bounds/microstructure relations*

Improved bounds are bounds that depend *nontrivially* upon two-point and high-order correlation functions and thus involve information beyond that contained in the volume

fractions. In the cases of the conductivity and elastic moduli of isotropic materials, for example, improved bounds are those which are tighter than the Hashin–Shtrikman bounds (Hashin and Shtrikman, 1962, 1963). Improved bounds on a variety of different effective properties have been derived in terms of $S_n(\mathbf{x}^n)$, i.e. the probability of finding n points at positions $\mathbf{x}^n \equiv \mathbf{x}_1, \ldots, \mathbf{x}_n$ in one of the phases (Prager, 1963; Beran, 1968; McCoy, 1970; Milton, 1982; Milton and Phan-Thien, 1982; Berryman and Milton, 1985; Rubinstein and Torquato, 1988; Torquato, 1991). For example, Silnutzer (1972) derived three-point bounds on the effective axial shear modulus μ_e of any transversely isotropic two-phase composite in terms of integrals over S_1, S_2, and S_3. Milton (1982) obtained corresponding four-point bounds. Although such three- and four-point bounds can provide significant improvement over two-point bounds, the bounds diverge as the contrast between the phase properties increases. The upper bound, for example, generally diverges to infinity when phase 2 is super-rigid relative phase 1, even if phase is topologically disconnected. The reason for this behavior is that *lower-order* S_n (see Fig. 1) do not reflect information about *percolating clusters or connected paths* in the system and accordingly bounds involving such lower-order information are referred to as *conventional* improved bounds.

Nonetheless, it is important to emphasize that it has been established (Torquato, 1991) that one of the bounds can still provide a good estimate of the properties in high-contrast situations, depending on whether the system is above or below the *percolation threshold*, i.e. the point at which a disconnected phase becomes connected. For example, Fig. 2 compares two-point (dotted curve), three-point (dashed curve), and four-point (solid curve) lower bounds on the effective axial shear modulus μ_e [computed by Torquato and Lado (1992)] to "exact" Brownian-motion simulation data (Kim and Torquato, 1990) in the extreme case of infinitely rigid fibers ($G_2/G_1 = \infty$). Even though the upper bounds diverge to infinity in this instance, the four-point lower bound provides a good estimate of the data since the cylindrical fibers do not form clusters (Torquato, 1991).

Conventional bounds on effective properties have been given in terms of other types of statistical quantities, including point/q-particle functions G_n ($n = 1+q$) (Torquato, 1986a) and surface–void F_{sv} and surface–surface F_{ss} correlation functions (Doi, 1976; Rubinstein and Torquato, 1988, 1989). Very recently, bounds on the effective thermal conductivity of suspensions of spheres with *imperfect interfaces* were derived in terms of related surface correlation functions (Torquato and Rintoul, 1995).

The aforementioned derived of conventional bounds in extreme instances notwithstanding, it highly desirable to derive sharper bounds in terms of morphological

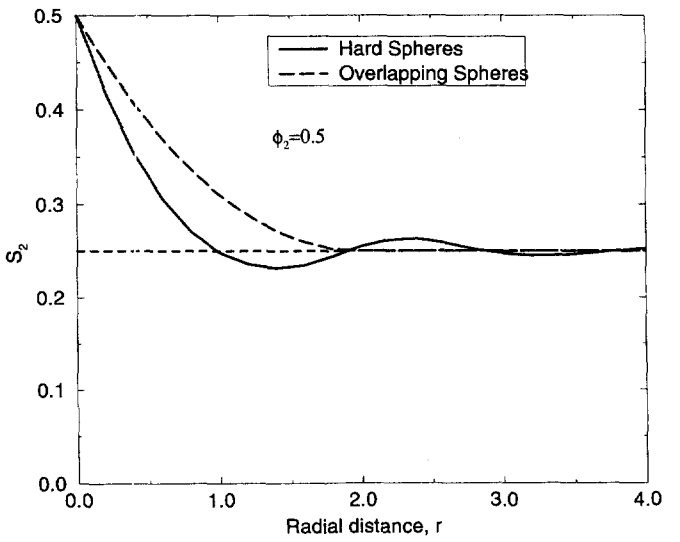

Fig. 1. The two-point probability function $S_2(r)$ vs radial distance r for nonoverlapping and overlapping spheres of unit diameter taken from Torquato (1991). Unlike the two-point cluster function $C_2(r)$, $S_2(r)$ does not contain connectedness information.

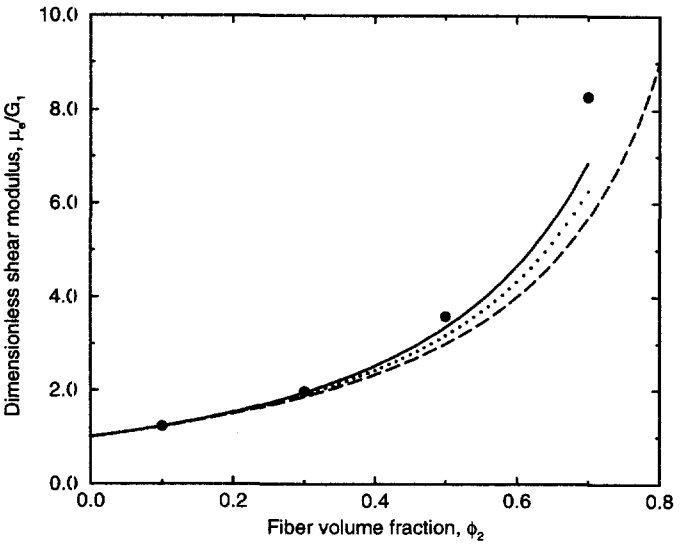

Fig. 2. Dimensionless effective axial shear modulus μ_e/G_1 vs fiber volume fraction ϕ_2 for random arrays of oriented cylindrical fibers in a matrix (G_1 is the matrix shear modulus). The fibers are superrigid relative to the matrix. Dashed, dotted and solid curves are two-, three-, and four-point lower bounds, respectively. Note that even though the upper bound diverges to infinity in this instance, the exact data (filled circles) lie close to the four-point lower bound.

quantities that better reflect percolation or connectedness information. Such bounds have been recently derived and computed by Torquato and Rubinstein (1991) and by Bruno (1991), using similar approaches, for the problem of conduction in particle suspensions. Letting σ_i be the conductivity of phase i, they were able to derive an upper bound on the effective conductivity σ_e which remained finite, in general, in the limit $\sigma_e/\sigma_1 \to \infty$ by incorporating information that the superconducting particles did not touch. Similarly, they found lower bounds on σ_e which did not necessarily vanish in the limit $\sigma_e/\sigma_1 \to 0$. Whereas Bruno's bounds involve the minimum distance between all particle pairs, the Torquato–Rubinstein bounds incorporate the nearest-neighbor distribution function $H_P(r)$. Bounds involving $H_P(r)$ have also been derived for the mean survival time (Rubinstein and Torquato, 1988) and the fluid permeability (Rubinstein and Torquato, 1989).

The Rubinstein–Torquato variational principle for the lower bound on the mean survival time τ for $\kappa = \infty$ has been generalized by Torquato and Avellaneda (1991) to treat the case of finite surface rate constant κ. Using this principle, Torquato and Avellaneda derived a lower bound on τ in terms of the first moment of *pore size distribution function* $P(r)$. $P(r)\,dr$ is the probability that a point in the pore region $\mathcal{V}_1$ lies at a distance between r and $r+dr$ from the nearest point on the interface $\partial\mathcal{V}$. This function contains some connectedness information.

2.2. *Microstructure characterization*

The previous section described some of the different types of statistical correlation functions ($S_n, G_n, F_{sv}, F_{ss}, H_P, P$) that have arisen in rigorous bounds on effective properties (Torquato, 1991). Until recently, application of such bounds (although in existence for almost 30 years in some cases) was virtually nonexistent because of the difficulty involved in ascertaining the correlation functions. Are these different functions related to one another? Can one write down a single expression that contains complete statistical information? The answers to these two queries are in the affirmative.

For statistically inhomogeneous systems of N identical d-dimensional spheres, Torquato (1986b) has introduced the general n-point distribution function $H_n(\mathbf{x}^m; \mathbf{x}^{p-m}; \mathbf{r}^q)$, which is defined to be the correlation associated with finding m points with positions $\mathbf{x}^m$ on certain surfaces within the medium, $p-m$ with positions $\mathbf{x}^{p-m}$ in certain spaces exterior to the spheres, and q sphere centers with positions $\mathbf{r}^q$, $n = p+q$. He also found a series

representation of H_n which enables one to compute it. From the general quantity H_n one can obtain all of the afore-mentioned correlation functions and their generalizations. This formalism has been generalized to treat polydispersed spheres (Lu and Torquato, 1991), anisotropic media (e.g. aligned ellipsoids and cylinders) (Torquato and Sen, 1990; Lado and Torquato, 1990) and cell models (Lu and Torquato, 1990b).

We should mention that quantities that are superb signatures of clustering and connectedness have been studied and quantified. These include the pair-connectedness function $P_2(r)$ (Coniglio *et al.*, 1977; Chiew *et al.*, 1985; Stell, 1984) and two-point cluster function $C_2(r)$ (Torquato *et al.*, 1988). The reader is referred to the review of Torquato (1991) for further details.

2.3. *Cross-property bounds*

An intriguing fundamental as well as practical question is the following: Can different properties of the heterogeneous material be *rigorously* linked to one another? Such cross-property relations become especially useful if one property is more easily measured than another property. Indeed, in the case of flow in porous media, the fluid permeability k is difficult to measure *in situ*. Thus, any indirect measurement that can be made *in situ* to ascertain k has great value. The same is true for relations that link the effective conductivity and effective elastic moduli.

Rigorous relations have been obtained that connect the fluid permeability k to diffusion parameters (Torquato, 1990; Avellaneda and Torquato, 1991; Torquato and Kim, 1992), such as the mean survival time τ (obtainable from an NMR measurement) and the effective electrical conductivity σ_e of a porous medium containing a conducting fluid of electrical conductivity σ_1 and an insulating solid phase.

Can the overall thermal (electrical) response of a heterogeneous medium to an applied thermal (electrical) load be related rigorously to the overall linear mechanical response of the same medium to an applied mechanical load? The answer is in the affirmative. Milton (1984), Berryman and Milton (1988) and Torquato (1992) obtained the first rigorous cross-property bounds that link conductivity and elastic moduli. Subsequently, these results were improved upon by Gibiansky and Torquato using the so-called *translation method* (Gibiansky and Torquato, 1993, 1995, 1996a). How sharp are these cross-property estimates given an exact determination of one of the effective properties? To examine this question, one can utilize exact results for the effective conductivity (Perrins *et al.*, 1979) and effective bulk modulus K_e (Eischen and Torquato, 1993) of hexagonal arrays of superconducting, superrigid inclusions (phase 2) in a matrix. Agreement between the Gibiansky–Torquato cross-property bounds and the exact elastic-moduli data is remarkably good (see Fig. 3). It is noteworthy that *standard variational upper bounds* on the effective properties (such as Hashin–Shtrikman) here diverge to infinity as they do not incorporate information that the superrigid phase is in fact disconnected. By contrast, our cross-property upper bound uses the fact that the infinite-contrast phase is disconnected via conductivity information.

Gibiansky and Torquato (1996b) have found bounds on the effective elastic moduli of cracked media in terms of the effective conductivity of such media. These represent the first nontrivial bounds on the effective properties of cracked media which are independent of the shapes and spatial distribution of the cracks. Cracks in a solid body can be considered to be a particular limiting case of inclusions in a matrix in the limit when the moduli and conductivity of the included phase and the inclusion volume fraction tend to zero. In this distinguished limit, all conventional bounds on the effective properties of heterogeneous media (e.g. Hashin–Shtrikman bounds) fail to deliver any useful results. The microgeometries of cracks that satisfy the bounds exactly are identified.

2.4. *Influence of spatial variability on failure of composites*

It is of great practical interest to understand how spatial variability in the microstructure of composites affects the failure characteristics of the heterogeneous materials (see Fig. 4). An in-depth summary of this important topic is beyond the scope of this paper. The reader is referred to Duxbury and Leath (1994), Ostoja-Starzewski *et al.* (1994), Haubensack *et al.* (1995), Zhou and Curtin (1995) and references therein for further

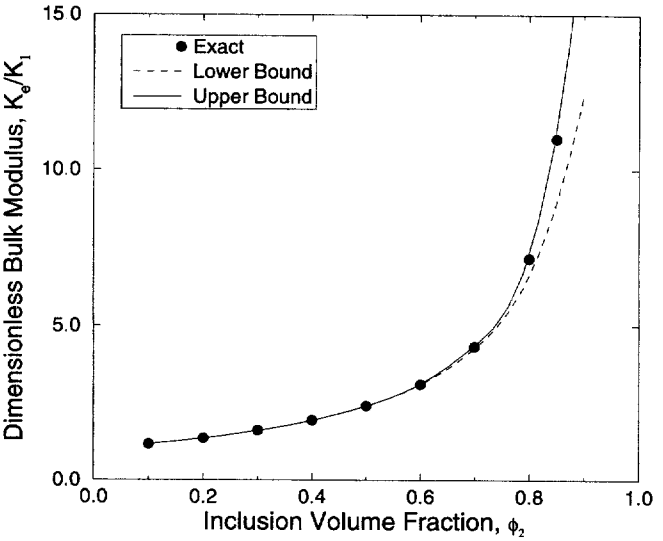

Fig. 3. Comparison of cross-property bounds on the dimensionless effective bulk modulus K_e/K_1 (curves) with exact data (Eischen and Torquato, 1993) for hexagonal arrays of superconducting, super-rigid inclusions. Here K_1 is the matrix bulk modulus.

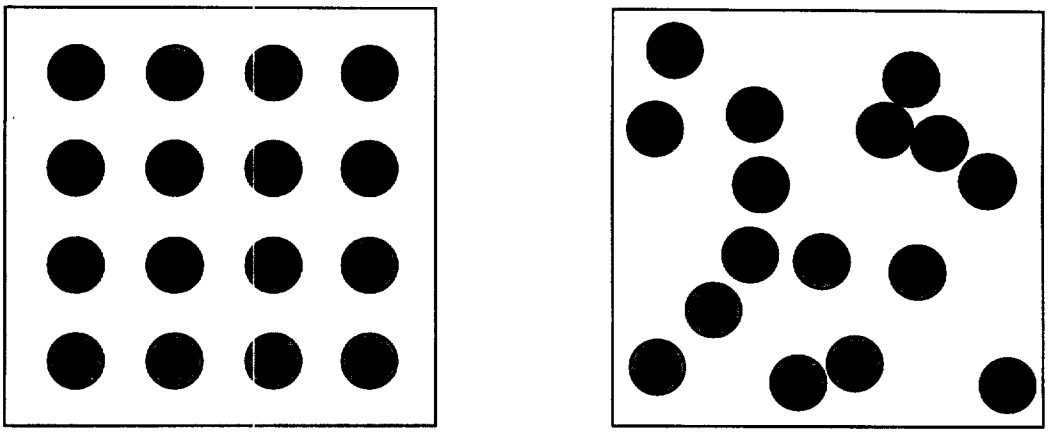

Fig. 4. Two systems at the same volume fraction, but the right-most example has greater fluctuations. The failure characteristics of these systems can be dramatically different from one another.

discussion. Here we motivate the need for quantitative characterization of microstructure fluctuations by discussing the salient failure mechanisms for three different examples reported in the literature.

The first concerns matrix cracking in fiber-reinforced ceramic composites. Barsoum *et al.* (1992) reported data on strength vs fiber spacing for borosilicate glass reinforced with SiC fibers under three-point bending. It was found that matrix cracks initiated at a lower stress as the local fiber spacing increased. Thus, the important length scale is the largest inter-fiber spacing, i.e. the extreme statistics govern the strength. This implies that naive attempts to estimate the strength using a simple rule of mixture relation must necessarily fail since volume fraction information is equivalent to average fiber spacing. Botsis *et al.* (1995) subsequently showed that a Griffith-type scaling relation for the strength involving the largest interfiber spacing provided good correlation with the data.

In another experimental study, MacKay (1990) investigated cracking in unidirectional metal matrix composites under thermal cycling. It was found that residual stresses caused

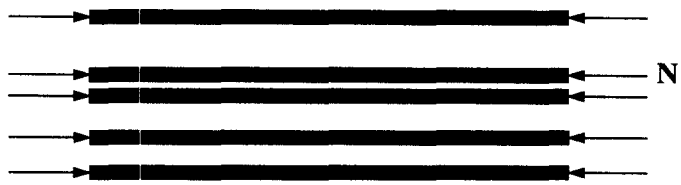

Fig. 5. A fiber composite modeled as a two-dimensional lamellar material consisting of fiber and matrix plates. N is the external compressive load.

matrix cracks and interfacial debonding. Cracking was related to the fiber distribution; more cracking occurred between the more closely spaced fibers within a row.

Finally, the last example concerns a theoretical study on the compressive strength of unidirectional composites by Chung and Weitsman (1994). In their model, random fiber spacing instigated the formation of severe transverse loadings on the fibers. The analysis required the probability density of fiber spacing $p(x)$ for the model depicted in Fig. 5. They chose to model the statistics by a Voronoi cell tesselation, which is somewhat artificial and unnecessary. An exact solution is described below, however.

We see from these three examples that spatial fluctuations in the microstructure can have important consequences for the failure characteristics of composites. Microstructure fluctuations is a topic of a long-standing interest in the statistical physics community, but much of this work has not permeated the applied mechanics or materials sciences communities. Indeed, new developments are still taking place within the statistical physics community. We will discuss some of our recent work along these lines focusing on *statistics of interfiber spacing* and *local volume fraction fluctuations* within an "observation" window.

Using the machinery of statistical mechanics, we have developed analytical expressions for probability density for interfiber spacing $p(x)$ for several models (Torquato and Lu, 1993), including the one depicted in Fig. 5. For this latter case of random impenetrable fibers of unit diameter at fiber volume fraction ϕ_2, we have found the exact relation

$$p(x) = \frac{\phi_2}{1-\phi_2} \exp\left[-\frac{\phi_2(x-1)}{1-\phi_2}\right].$$

This function is plotted in Fig. 6 for two different volume fractions. Of course, there are many other measures of interfiber or interparticle distances [such as the nearest-neighbor

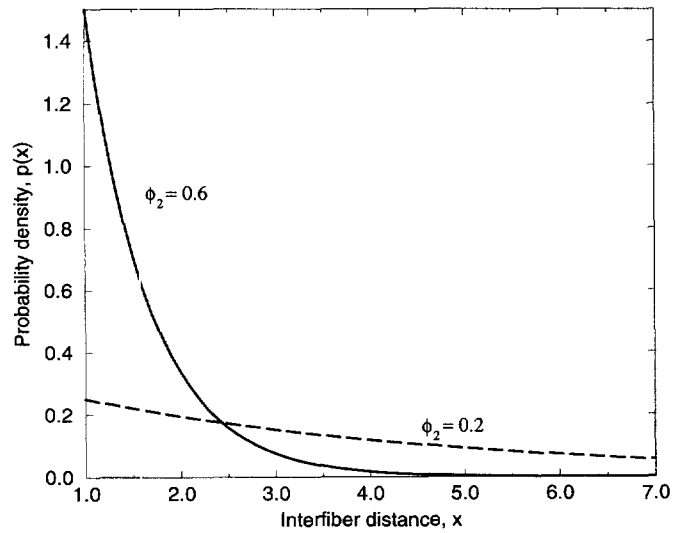

Fig. 6. Probability density function $p(x)$ interfiber spacing x for two different values of fiber volume fraction ϕ_2 for the model depicted in Fig. 5.

distribution function (Torquato, 1995)] which we will not be able to describe here in any detail.

Although the volume fraction is a constant for a statistically homogeneous random medium, on a spatially local level it fluctuates and hence is a random variable ξ for a given "window" size (see Fig. 7). The coarseness C (Lu and Torquato, 1990a) is defined such that

$$C = \frac{\sqrt{\langle \xi^2 \rangle - \langle \xi \rangle^2}}{\langle \xi \rangle}$$

where angular brackets denote an ensemble average. The coareseness provides a measure of the uniformity of coverage of the phases. For infinitely large observation window volume V_0, C must tend to zero. The coarseness C can be used to quantitatively determine the minimum length scale over which fluctuations can be regarded to be sufficiently small (see Fig. 7).

For *general anisotropic* media (Lu and Torquato, 1990a), it can be shown that

$$C = \frac{1}{\phi_1 V_0} \left\{ \int [S_2(\mathbf{r}) - \phi_1^2] v_2^{\text{int}}(\mathbf{r}) \, d\mathbf{r} \right\}^{1/2}.$$

Here S_2 is two-point probability function and $v_2^{\text{int}}(\mathbf{r})$ is intersection volume of two observation regions whose centroids are separated by the displacement $\mathbf{r}$. Thus, the coarseness can be determined by measuring S_2 and then performing the integration above. It also can be measured directly from micrographs of the material. Lu and Torquato (1990a) computed C for a variety of model microstructures.

To further study local fluctuations in the volume fractions, we have calculated recently all of the moments of ξ or, equivalently, the full distribution of ξ for several models of random media using analytical and simulation methods (Quintanilla and Torquato, 1997a). Generally, the probability distribution is not Gaussian (normal). We determined the conditions under which ξ can be reasonably approximated by a normal distribution, i.e. when the coarseness C characterizes the fluctuations well.

We should note that one can also define a local effective property value for a given window and hence examine local property fluctuations. The reader is referred to Ostoja-Starzewski (1994) as an example of such a study in which the effective elastic moduli were computed numerically.

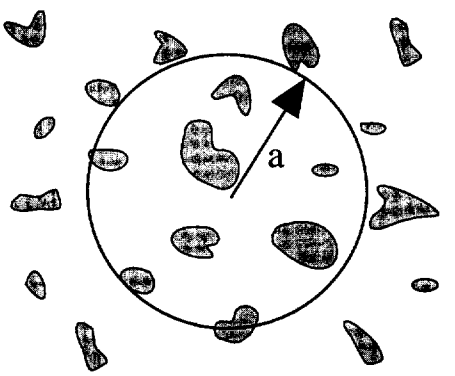

Fig. 7. Depiction of a spherical observation window of radius a at a particular point in a random medium. Clearly the matrix volume fraction contained within the window will fluctuate from point to point.

3. STRUCTURE AND PROPERTIES OF STATISTICALLY INHOMOGENEOUS MEDIA

The preponderance of previous work on heterogeneous media assumes statistical homogeneity. Significantly less research has been devoted to the study of *statistically inhomogeneous* random media. In such instances, ergodicity is lost; that is, one cannot equate ensemble and volume averages. Moreover, the n-point correlation functions are no longer translationally invariant, implying that they depend upon the absolute positions of the n points. For example, the probability of finding a point in phase i at position $\mathbf{x}$ or, equivalently, the volume fraction of phase i, $\phi_i(\mathbf{x})$, now depends on the position $\mathbf{x}$. (This is in contrast to homogeneous media in which $\phi_i(\mathbf{x})$ is a constant.) One simple example of a statistically inhomogeneous medium is any two-phase system which is defined on a finite region. Although most applications permit $\phi_1(\mathbf{x})$ to vary in only one direction, it can be chosen to be any function in principle. However, defining a two-phase medium on an infinite region does not preclude statistical inhomogeneity. Physical examples of statistically inhomogeneous, two-phase media include, composites in which the heterogeneity length scale is not much smaller than the macroscopic size of the sample, functionally graded materials [see Abboud *et al.* (1994); Fukui *et al.* (1994); Cherradi *et al.* (1994); Zuiker and Dvorak (1994); Reiter *et al.* (1997); Nadeau and Ferrari (1995)] porous media with spatially variable fluid permeability (Gelhar, 1993), and distributions of galaxies (Bond *et al.*, 1996).

3.1. *Model of inhomogeneous fully penetrable spheres*

Following the development of the study of the microstructure and properties of homogeneous random media, we propose a microstructural model for particulate, statistically inhomogeneous two-phase random media in this paper. This model is a two-phase system consisting of an *inhomogeneous distribution of fully penetrable spheres* in space whose particle density obeys *any specified variation in volume fraction*. The space exterior to the spheres is called phase 1, and phase 2 is the space occupied by the spheres. This inhomogeneous model is nontrivial in that cluster formation naturally arises and it permits significantly more complicated microstructures than the aforementioned layered models. Four two-dimensional realizations of this model with different grades are shown in Fig. 9.

We will consider D-dimensional space $\mathscr{R}^D$ as our measurable space. We also assume that ν is a *measure* on $\mathscr{R}^D$ so that the measure νB of any measurable set B with respect to ν is given by

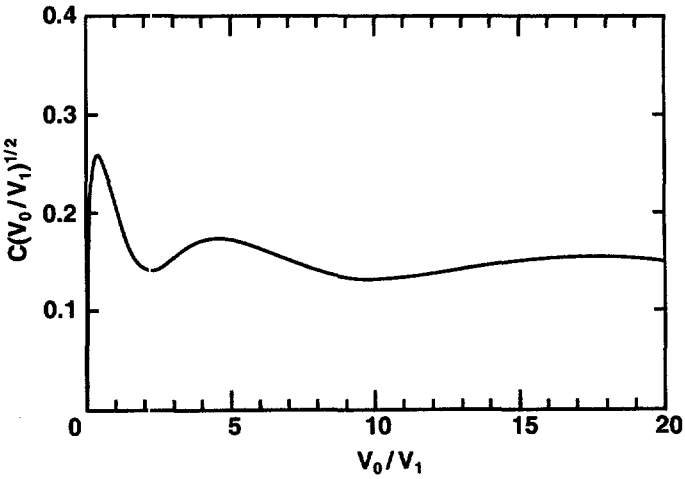

Fig. 8. The coarseness C multiplied by the asymptotic long-range value of $(V_0/V_1)^{1/2}$ vs the ratio V_0/V_1 for random impenetrable spheres in matrix, where V_0 and V_1 are the volumes of the observation window and inclusion, respectively [taken from Lu and Torquato (1990a)]. The range over which $C(V_0/V_1)^{1/2}$ oscillates can be used to determine the minimum length scale over which fluctuations can be regarded to be sufficiently small.

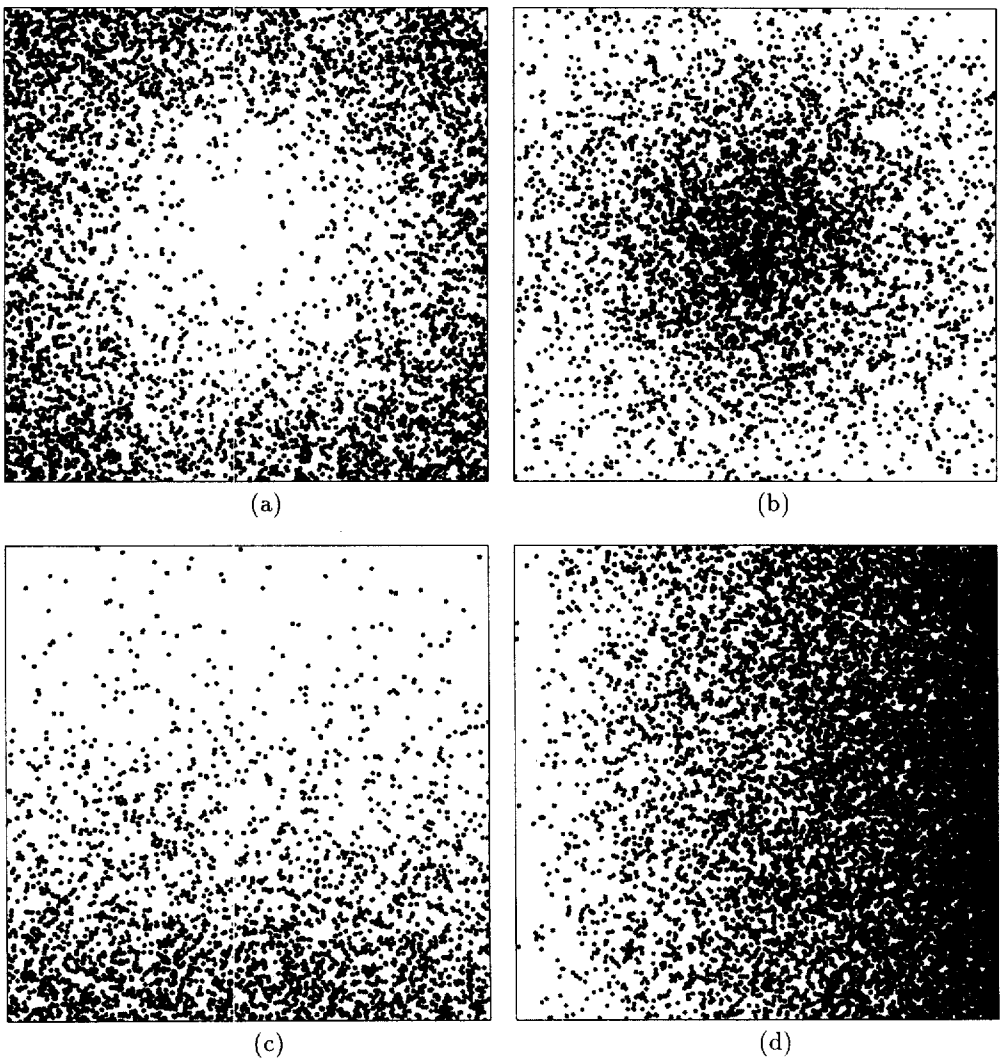

Fig. 9. Four realizations of statistically inhomogeneous fully penetrable disks. System (a) may be thought of as arising from a centrifugal field, while system (b) can be viewed as a system in an "anti-centrifugal" field. System (c) is one under a constant gravitational field in the vertical direction, whereas system (d) has a linear grade in the volume fraction in the horizontal direction. The density functions of systems (a)–(d) are given by (5)–(8), respectively, with parameters that are given in the text.

$$\nu B = \int_B \rho(\mathbf{x})\, d\mathbf{x} \tag{1}$$

for some function ρ on $\mathscr{R}^D$. When $\rho(\mathbf{x}) = 1$ for all $\mathbf{x}$, the measure ν is ordinary Lebesgue measure and, hence, νB is simply the volume of B. Condition (1) is satisfied if ν is absolutely continuous to Lebesgue measure (Royden, 1988).

A *general Poisson process* $\mathcal{N}$ with intensity measure ν is defined to be a point process which satisfies the following two properties (Stoyan *et al.*, 1995):

(i) The number of points in a bounded Lebesgue set B has any Poisson distribution with mean νB, that is, for $m = 0, 1, 2, \ldots$,

$$Pr(\mathcal{N}(B) = m) = \frac{(\nu B)^m}{m!} e^{-\nu B}. \tag{2}$$

(ii) For all $n \geq 2$, the random variables $\mathcal{N}(A_1), \ldots, \mathcal{N}(A_n)$ are independent whenever the Lebesgue sets $A_1, \ldots, A_n$ are pairwise disjoint.

The density $\rho(\mathbf{x})$ is called the *density function* of $\mathcal{N}$; this function will be used often in this paper. It is important to note that if $\rho(\mathbf{x}) = \rho$, a constant, then a general Poisson process reduces to an ordinary Poisson process with number density (or intensity) ρ. However, even if $\rho(\mathbf{x})$ is not constant, it has an appealing intuitive interpretation: $\rho(\mathbf{x})\,d\mathbf{x}$ is the probability that there is a point of $\mathcal{N}$ in an infinitesimal region $d\mathbf{x}$ about $\mathbf{x}$.

We notice from condition (i) that the probability that a region B contains no points of $\mathcal{N}$ is

$$Pr(\mathcal{N}(B) = 0) = e^{-\nu B} = \exp\left[-\int_B \rho(\mathbf{x})\,d\mathbf{x}\right]. \tag{3}$$

This calculation of the *exclusion probability* for B will be used repeatedly for different sets B in the calculations of Section 4.

We also notice that this general framework can be used to define systems on a *finite* region $\mathcal{R}$ by choosing the intensity function to be the restriction of ρ to $\mathcal{R}$, that is,

$$\rho_{\mathcal{R}}(\mathbf{x}) = \begin{cases} \rho(\mathbf{x}), & \mathbf{x} \in \mathcal{R}, \\ 0, & \text{otherwise.} \end{cases} \tag{4}$$

The microstructure functions for such finite systems are then calculated by using $\rho_{\mathcal{R}}$ in place of ρ.

Simulating realizations of general Poisson processes can be easily done in two stages if the density function $\rho(\mathbf{x})$ is bounded on $\mathcal{R}^D$ (Stoyan *et al.*, 1995), say $\rho(\mathbf{x}) \leqslant \rho^*$. First, a Poisson process of density ρ^* is simulated. Second, the resulting point pattern is thinned. Each point $\mathbf{x}$, independently of the other points, is kept with probability $\rho(\mathbf{x})/\rho^*$ or deleted with probability $1-\rho(\mathbf{x})/\rho^*$. The resulting point pattern is a general Poisson process with intensity function $\rho(\mathbf{x})$. This construction may be enhanced by partitioning $\mathcal{R}^D$ into regions in which $\rho(\mathbf{x})$ does not vary significantly. Finally, we place spheres of common radius R on the points of $\mathcal{N}$ to construct a realization of inhomogeneous fully penetrable spheres.

Four examples of the density function are given as follows:

$$\text{(a)} \quad \rho(x,y) = C\left(\frac{r\lambda L}{R}\right)^2, \tag{5}$$

$$\text{(b)} \quad \rho(x,y) = \frac{C}{R^2}\exp\left(-\frac{r\lambda}{L}\right), \tag{6}$$

$$\text{(c)} \quad \rho(x,y) = \frac{C}{R^2}\exp\left(-\frac{y\lambda}{L}\right), \tag{7}$$

$$\text{(d)} \quad \rho(x,y) = \frac{C}{R^2}\ln\left(\frac{[1+\varepsilon]\lambda}{[1+\varepsilon]L-x}\right), \tag{8}$$

respectively. Here r is the distance from a fixed point (say the center of the system), C is a multiplicative factor, L is the length scale of the entire system, λ is the length scale of the grade in volume fraction, and ε is very small. For all of these systems, the origin is placed at the lower-left corner. As discussed above, the value of the density function $\rho(\mathbf{x})$ at a given point $\mathbf{x}$ is directly correlated to the average density of centers around $\mathbf{x}$. The systems generated by these density functions may be thought of as arising from special external fields. System (a) may be thought of as arising from a centrifugal field, while system (b) can be viewed as a system in an "anti-centrifugal" field. System (c) is one under a constant gravitational field in the vertical direction, whereas, as we will show in Section 4, system (d) has a linear grade in the volume fraction in the horizontal direction, given by

$$\phi_1(x) \approx \frac{(1+\varepsilon)L - x}{(1+\varepsilon)\lambda}. \tag{9}$$

Other systems with different grades in volume fractions can also be constructed with different choices of the density function $\rho(\mathbf{x})$.

Note that there are *three* length scales associated with these systems: the size of the particles R, the size of the region L, and the length scale λ of the variation of $\rho(x, y)$. Even if the region is taken to be infinite, there will still be two length scales for these systems, namely, R and λ. This is in contrast to homogeneous two-phase random media on infinite domains, which possess only the length scale of the particles. We again note that statistically inhomogeneous systems are not ergodic and hence ensemble averages cannot be equated with volume averages.

In Fig. 9 we present realizations of inhomogeneous fully penetrable disks with density functions given by (5)–(8). Although only two-dimensional realizations are presented, the simulation procedure may be used in higher dimensions as well. For all four systems (a)–(d), the size of the particles is $R = 1$, and the macroscopic system size is $L = 200$. We also use the following parameters to generate Fig. 9:

$$\text{(a)} \quad C = 0.8, \quad \lambda = 1, \tag{10}$$

$$\text{(b)} \quad C = 0.6, \quad \lambda = 5, \tag{11}$$

$$\text{(c)} \quad C = 0.3, \quad \lambda = 4, \tag{12}$$

$$\text{(d)} \quad C = 1/\pi, \quad \lambda = L. \tag{13}$$

We also notice that the maximum volume fraction of phase 2 in system (d) is $\phi_2 \approx 1$ along the right edge, but the maximum particle volume fraction for (c) is roughly $\phi_2 \approx 0.6$ on the bottom edge.

We see in these figures that even the concept of volume fraction has lost its simplicity: the probability that a point lies in a sphere is dependent on the absolute location of the point. In fact, all of the usual microstructure functions will depend on the absolute positions of the arguments. Nonetheless, the general theory of Poisson processes can be employed to characterize the microstructure of inhomogeneous fully penetrable spheres.

3.2. *Calculation of the microstructure functions*

In this section, we summarize the procedure used by Quintanilla and Torquato (1997b) to obtain the general n-point distribution function H_n in the special case of statistically inhomogeneous fully penetrable spheres. From this relation we can then compute any of the correlation functions that have arisen in rigorous bounds on the effective properties of such media. For purposes of illustration, we focus on obtaining the n-point probability function S_n for phase 1, the nearest-neighbor functions E and H, and the lineal-path function L.

Torquato (1986b) calculated the general n-point distribution function for homogeneous fully penetrable spheres and found

$$H_n(\mathbf{x}^m; \mathbf{x}^{p-m}; \mathbf{r}^q) = (-1)^m \rho^q \exp[-\rho V_p(\mathbf{x}^p; a^p)] \frac{\partial}{\partial a_1} \cdots \frac{\partial}{\partial a_m} \prod_{l=1}^{q} \prod_{k=1}^{p} e(y_{kl}; a_k)$$
$$+ (-1)^m \rho^q \prod_{l=1}^{q} \prod_{k=1}^{p} e(y_{kl}; a_k) \frac{\partial}{\partial a_1} \cdots \frac{\partial}{\partial a_m} \exp[-\rho V_p(\mathbf{x}^p; a^p)]. \tag{14}$$

In this expression, $V_p(\mathbf{x}^p; a^p)$ is the union volume of p spheres of radii $a^p \equiv a_1, \ldots, a_p$ centered at $\mathbf{x}_1, \ldots, \mathbf{x}_p$, respectively, $y_{ij} = |\mathbf{x}_i - \mathbf{r}_j|$ and

$$e(y;a) = \begin{cases} 0, & y \leqslant a, \\ 1, & y > a. \end{cases} \tag{15}$$

The calculation of H_n for statistically inhomogeneous fully penetrable sphere is a bit more involved, but we have noticed that the inhomogeneous result can be obtained from the homogeneous expression (14) with the following replacements:

$$\rho^q \to \rho(\mathbf{r}_1), \ldots, \rho(\mathbf{r}_q) \quad \text{and} \tag{16}$$

$$\rho V_p(\mathbf{x}^p; \alpha^p) \to \int_{V_p(\mathbf{x}^p;\alpha^p)} \rho(\mathbf{r})\, d\mathbf{r}, \tag{17}$$

where $\rho(\mathbf{r})$ is a position-dependent number density of inclusions.

The n-point function S_n can be obtained from the H_n following the prescription given in Torquato (1986b). Specifically, we find that

$$S_n(\mathbf{x}^n) = \exp\left[-\int_{V_n(\mathbf{x}^n;R)} \rho(\mathbf{r})\, d\mathbf{r}\right], \tag{18}$$

where $V_n(\mathbf{x}^n; R)$ is the union of n spheres with common radius R centered at $\mathbf{x}^n$. In particular, the one-point probability function $S_1(\mathbf{x})$, equal to the volume fraction $\phi_1(\mathbf{x})$ of phase 1, is given by

$$S_1(\mathbf{x}) = \exp\left[-\int_{V_1(\mathbf{x};R)} \rho(\mathbf{r})\, d\mathbf{r}\right]. \tag{19}$$

In Fig. 10, S_1 is plotted for system (d), the linear-grade model of Fig. 9. Recall that the radii of the disks is unity and the side length of the square is 200 and the origin is placed at the lower-left corner of system (d). We present graphs of S_2 for this same density function in Fig. 11. We see that $S_2(\mathbf{x}_1, \mathbf{x}_2)$ is dependent on both the absolute positions of $\mathbf{x}_1$ and $\mathbf{x}_2$, expressed in this figure through the location of $\mathbf{x}_1$ and the distance and direction of the displacement $\mathbf{x}_2 - \mathbf{x}_1$. We also see that S_2 increases somewhat as θ increases from 0 to $\pi/2$. This is intuitively clear since the volume fraction of phase 1 decreases as the x-coordinate increases.

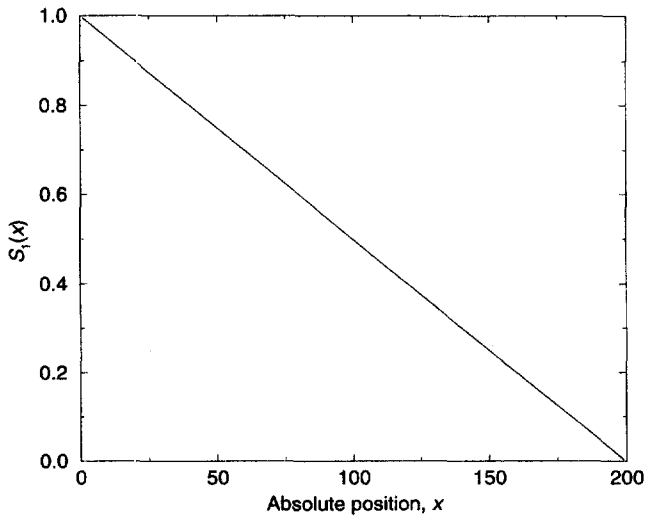

Fig. 10. Phase 1 volume fraction $\phi_1(x) = S_1(x)$ vs position x for system (d) of Fig. 9, calculated from (19). The grade in volume fraction is approximately given by $\phi_1(x) = 1 - x/L$.

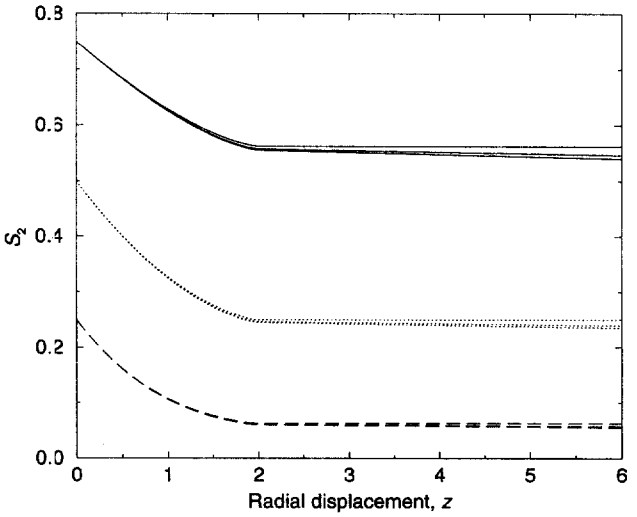

Fig. 11. The two-point probability function $S_2(\mathbf{x}_1, \mathbf{x}_2)$ vs radial distance $z = |\mathbf{x}_2 - \mathbf{x}_1|$ for system (d) of Fig. 9. The x-coordinate of $\mathbf{x}_1$ is chosen to be 50 (solid lines), 100 (dotted lines), and 150 (dashed lines); recall that the side length of the box is $L = 200$. In each set of lines, the lowest line corresponds to $\theta = 0$ [where $\mathbf{x}_2 - \mathbf{x}_1 = (z\cos\theta, z\sin\theta)$], the middle to $\theta = \pi/4$, and the highest to $\theta = \pi/2$. As expected, S_2 is dependent on the absolute positions of $\mathbf{x}_1$ and $\mathbf{x}_2$, not just the radial displacement.

The exclusion probabilities $E_V(\mathbf{x}; z)$ and $E_P(\mathbf{x}; z)$ (Torquato, 1991) can also be obtained from the general n-point function. The function $E_V(\mathbf{x}; z)$ is the probability that the sphere $V_1(\mathbf{x}; z)$ of radius z centered at a point $\mathbf{x}$ in the void phase contains no particle centers, while $E_P(\mathbf{x}; z)$ is the probability that the sphere contains no other particle centers given that $\mathbf{x}$ is a particle center. For homogeneous and inhomogeneous fully penetrable spheres, these probabilities are identical and will be referred to as $E(\mathbf{x}; z)$. Clearly, $E(\mathbf{x}; 0) = 1$ and $E(\mathbf{x}; R) = \phi_1(\mathbf{x})$. From relation (14) for H_n and the prescription relating H_n to E (Torquato, 1991), we find

$$E(\mathbf{x}; z) = \exp\left[-\int_{V_1(\mathbf{x};z)} \rho(\mathbf{r})\, d\mathbf{r}\right] \tag{20}$$

and similarly for $H(\mathbf{x}; z)$. Plots of E for the linear-grade model (d) of Fig. 9 are shown in Fig. 12. The *nearest-neighbor distribution function* (more accurately, probability density function) is defined from E by

$$H(\mathbf{x}; z) = -\frac{\partial E(\mathbf{x}; z)}{\partial z}. \tag{21}$$

The so-called lineal-path function $L(\mathbf{x}_1, \mathbf{x}_2)$, the probability that the line segment connecting $\mathbf{x}_1$ and $\mathbf{x}_2$ lies entirely in phase 1, was also calculated for this model. These results are presented in the work of Quintanilla and Torquato (1997b).

3.3. *Effective properties of statistically inhomogeneous media*

As alluded to earlier, for statistically inhomogeneous media in which there is a gradation of density, there are at least three characteristic length scales; the microscale R (e.g. size of particles or average interparticle distance), the gradation length scale λ, and the macroscopic length of the composite sample L. Consider the situation in which $L \gg \lambda > R$. Let the variable $\mathbf{x}$ describe variation on the macroscale ("slow scale") and $\mathbf{y} = \mathbf{x}/\varepsilon$ describe variation on the microscale ("fast scale"), where $\varepsilon = R/\lambda$. It is well known that if $\varepsilon \to 0$, then the homogenized constitutive relation (Sanchez-Palencia, 1980) will involve effective properties that will depend upon the position $\mathbf{x}$. In this distinguished limit, one can then

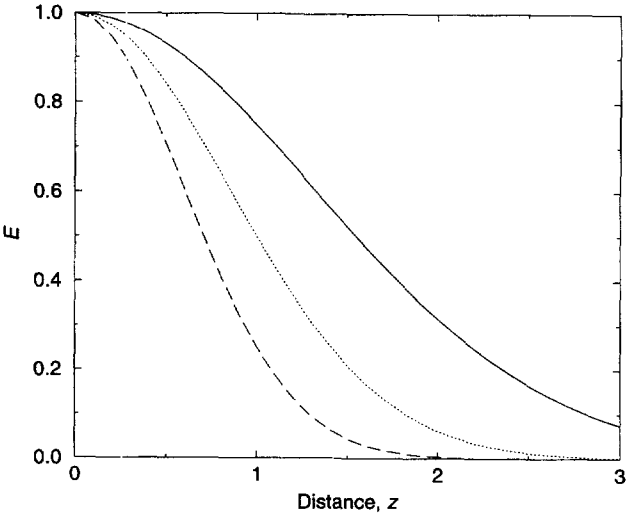

Fig. 12. The exclusion probability $E(\mathbf{x};z)$ vs radial distance z for system (d) of Fig. 9. The x-coordinate of $\mathbf{x}$ is chosen to be 50 (solid line), 100 (dotted line), and 150 (dashed line). We see that E is dependent upon the absolute position $\mathbf{x}$.

apply previous homogeneous effective-property estimates that incorporate volume-fraction information only (e.g. self-consistent approximations, Voigt–Reuss bounds, Hashin–Shtrikman bounds) by evaluating them at the position-dependent phase volume fraction $\phi_i(\mathbf{x})$. For example, the Voigt–Reuss bounds on the position-effective bulk modulus $K_e(\mathbf{x})$ are given by

$$K_e(\mathbf{x}) \leqslant K_1\phi_1(\mathbf{x}) + K_2\phi_2(\mathbf{x}), \tag{22}$$

$$K_e(\mathbf{x}) \geqslant \left[\frac{\phi_1(\mathbf{x})}{K_1} + \frac{\phi_2(\mathbf{x})}{K_2}\right]^{-1}. \tag{23}$$

Similarly, the three-dimensional Hashin–Shtrikman bounds on $K_e(\mathbf{x})$ for $K_2 \geqslant K_1$ and $G_2 \geqslant G_1$ are

$$K_e(\mathbf{x}) \leqslant K_1\phi_1(\mathbf{x}) + K_2\phi_2(\mathbf{x}) - \frac{(K_2-K_1)^2\phi_1(\mathbf{x})\phi_2(\mathbf{x})}{K_1\phi_2(\mathbf{x}) + K_2\phi_1(\mathbf{x}) + \frac{4}{3}G_2} \tag{24}$$

$$K_e(\mathbf{x}) \geqslant K_1\phi_1(\mathbf{x}) + K_2\phi_2(\mathbf{x}) - \frac{(K_2-K_1)^2\phi_1(\mathbf{x})\phi_2(\mathbf{x})}{K_1\phi_2(\mathbf{x}) + K_2\phi_1(\mathbf{x}) + \frac{4}{3}G_1}. \tag{25}$$

However, these formulas are, strictly speaking, not valid even when ε is small, but non-zero, i.e. the effective properties will no longer be scale-independent, but depend upon λ. Nonetheless, recently Reiter *et al.* (1997) have shown that the self-consistent and other approximate methods can provide reasonable estimates of the effective properties in those parts of graded composite materials with a well-defined continuous matrix and discontinuous reinforcement. Another situation in which formulas such as (22)–(25) will break down is when L is not much larger than λ or R. In this instance, it may not even be meaningful to speak about effective properties or, at best, there will be corrections to the effective properties that depend upon the sample size and boundary conditions.

4. RECONSTRUCTING RANDOM MEDIA: AN INVERSE PROBLEM

A very interesting problem in the image analysis of real heterogeneous media is the reconstruction problem, i.e. the generation of model microstructures that, at some level, has the same statistical properties as the real heterogeneous media. Having reconstructed the heterogeneous medium, one can then evaluate its effective properties (via direct simulations) and compare these values to experimentally measured transport properties of the actual porous medium. There are a few such studies in the literature, but a notable one is the work of Adler *et al.* (1990) who reconstructed sandstones using the standard two-point probability function $S_2(r)$ mentioned earlier. They found that the experimentally measured permeabilities were about five times larger than the reconstructed permeabilities. The reason for this large discrepancy is clear—$S_2(r)$ does not contain connectedness information about the pore space. A more general procedure is needed that is capable of incorporating other correlation functions, especially those that reflect connectedness information.

Rintoul and Torquato (1997) have very recently proposed a novel procedure to reconstruct the many-body systems from given structural information (see Fig. 13). Our procedure is a variation of the simulated annealing method that is commonly used to solve a variety of general problems relating to finding a state of minimum "energy" among a set of many local minima (Brooks and Morgan, 1995). The energy does not necessarily have to be a physical energy of the system, but can be any relevant objective function (e.g. time in a production process). The success of the reconstruction can be measured by how well

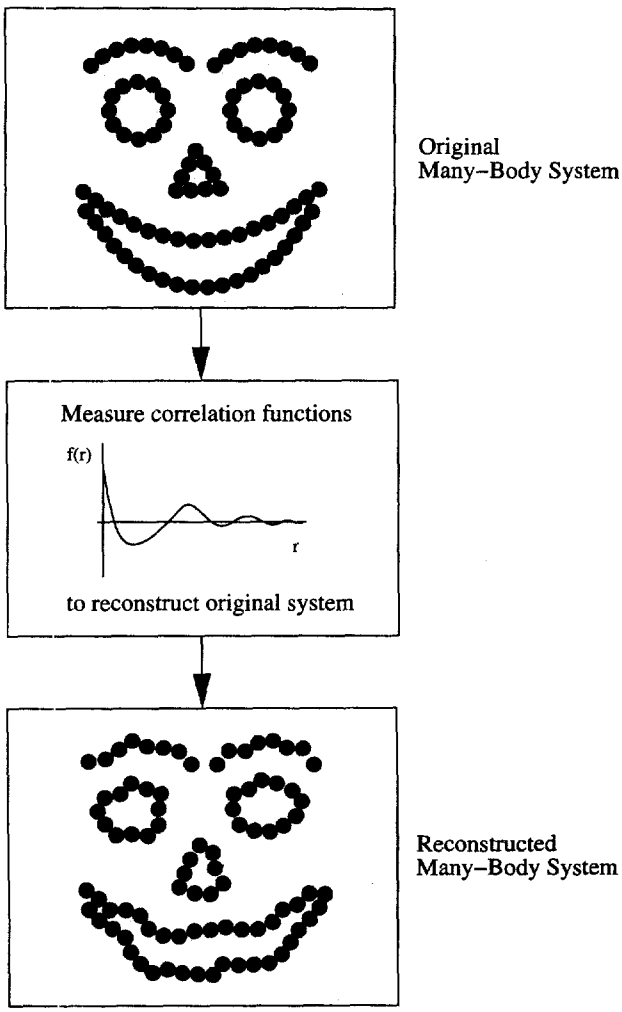

Fig. 13. Schematic of reconstruction process.

the reconstructed system reproduces not only the correlation functions from which the reconstruction was performed, but other correlation functions as well. Clearly, even if the correlation functions of the reference and reconstructed systems are in good agreement, this does not ensure that structures of the two systems will match very well. This interesting question of nonuniqueness can also be probed.

4.1. *Reconstruction procedure*

We first describe our reconstruction methodology by considering a single correlation function associated with the original, or "reference" system. For simplicity, we assume a reference two-point correlation function of the form $f_0(r)$ that depends only on the distance r between two points in the system. Examples of such correlation functions are the two-point probability function $S_2(r)$ (Torquato and Stell, 1985), radial distribution function $g(r)$ (Hansen and McDonald, 1986), pair-connectedness function $P_2(r)$ (Coniglio *et al.*, 1977), two-point cluster function $C_2(r)$ (Torquato *et al.*, 1988), and pore-size distribution function $P(r)$ (Torquato and Avellaneda, 1991). The reference function is the one that we will attempt to reproduce in a many-body system created via computer simulation. The same correlation function associated with the many-body system in the simulation will be denoted as $f_s(r)$ and it is this system which we will attempt to evolve towards $f_0(r)$. Because $f_s(r)$ of our simulated many-body system is based on the distribution of the distances between particles in a finite system, it is necessary to discretize $f_s(r)$ through a process of binning. In this process, the relevant values of the correlation functions at different inter-particle separation distances r_{ij} are calculated and are placed in equal sized bins of width w_b centered at r_k, such that

$$r_k - w_b/2 \leqslant r_{ij} < r_k + w_b/2. \tag{26}$$

Once $f_s(r)$ is known at the specific values of the bins, one can define a variable E which plays the role of the "energy" in the simulated annealing calculation as

$$E = \sum_i \beta_i (f_s(r_i) - f_0(r_i))^2, \tag{27}$$

where β_i is an arbitrary weight which is implicitly a function of r through its dependence on the ith bin, and the sum is over all bins. Defined in this manner, E has the property of decreasing when the difference between any two bins decreases. The variable β_i can be varied depending on whether one wants to weight small values of the radial distance r greater than larger values of r. This is sometimes useful since the small r values of $f_s(r)$ are more important in determining the system structure.

In order to evolve the system toward $f_0(r)$, we choose a particle i and give it a random displacement $\delta\mathbf{r}$. Then, the energy E' of this state is calculated. We can now calculate the energy difference between two states $\Delta E = E' - E$, and define the acceptance probability of the move $p(\Delta E)$ via the method originally proposed by Metropolis *et al.* (and used in many simulated annealing calculations) as

$$p(\Delta E) = \begin{cases} 1 & \Delta E \leqslant 0 \\ \exp(-\Delta E/kT) & \Delta E > 0. \end{cases} \tag{28}$$

This method causes $f_s(r)$ to move gradually closer to $f_0(r)$. The value of T is chosen to allow the system to evolve to the desired state as quickly as possible, without getting trapped in any local energy minimum. For most simulated annealing problems, T is varied as a function of time in the simulation in order to reach the desired result as quickly as possible. This variation of T as a function of time is known as the *cooling schedule*.

This procedure can be naturally generalized to a more complicated dependence on the positions of the particles. This is done by considering a reference n-point correlation function $f_0(\mathbf{r}^n)$, which depends upon n different positions $\mathbf{r}^n = \mathbf{r}_1, \ldots, \mathbf{r}_n$. Also, one can even

extend the process to m different n-point correlation functions by defining a reference function $f_0(\mathbf{r}^n)$, where

$$f_0(\mathbf{r}^n) = f_0^{(1)}(\mathbf{r}^n) + f_0^{(2)}(\mathbf{r}^n) + \ldots, + f_0^{(m)}(\mathbf{r}^n), \tag{29}$$

[and a similar accompanying $f_s(\mathbf{r}^n)$] giving an energy

$$E = \sum_i \beta_i (f_s(\mathbf{r}^n) - f_0(\mathbf{r}^n))^2, \tag{30}$$

where the sum is a multidimensional one over all bins, and again, β_i depends implicitly on $\mathbf{r}^n$ through the ith bin.

4.2. *Applications to many-particle systems*

We apply our formulation by considering a reconstruction of a non-equilibrium system created by the random sequential adsorption (RSA) process (Widom, 1966; Feder, 1980) in two dimensions. In this process disks are placed randomly and sequentially on a surface such that each disk is adsorbed if it does not overlap any of the disks already adsorbed. The geometrical blocking effects and the irreversible nature of the process results in structures that are distinctly different from corresponding equilibrium configurations, except for low densities (Widom, 1966). The jamming limit (the final state of this process whereby no particles can be added) occurs at a volume fraction $\phi \approx 0.55$ (Feder, 1980).

For the purposes of illustration, we specialize in this paper to the case when the reference correlation function is taken to be the well-known *radial distribution function* (RDF) $g(r)$. The quantity $\rho 2\pi r g(r)\,dr$ gives the average number of particle centers in an annulus of thickness dr at a radial distance of r from the center of a particle (where ρ is the number density). The RDF is of central importance in the study of equilibrium liquids in which the particles interact with pairwise-additive forces since all of the thermodynamics can be expressed in terms of the RDF. The RDF can be ascertained from scattering experiments, which makes it a likely candidate for the reconstruction of a real system. The use of the RDF implies that in eqn (27) $f_0(r) = g(r)$, i.e. the reference function is a single function that depends only on the interparticle distance r. The weight β_i used in this case was $1/r_i$. The RDF for a reference RSA system was obtained by averaging over 100 RSA systems of 50,000 disks at a disk volume fraction $\phi = 0.543$. The RDF was used for distances $1 \leqslant r/\sigma \leqslant 5$. Also, since the RSA system does not allow overlap, trial moves causing disks to overlap were rejected. We will attempt this reconstruction using a starting condition of 5000 random equilibrium disks. The simulated annealing temperature T was kept constant for the simulation. We found that a more complicated cooling schedule did not significantly speed the reconstruction process.

Figure 14 shows that the reference RDF and reconstructed RDF agree fairly well at $\phi = 0.543$ in the RSA system. There is a slight discrepancy near the minima and maxima of the original RDF, with the peaks being slightly larger in the reconstructed RDF. The reason for this is partially due to the finite temperature used in the reconstruction. This temperature, which allows some moves to occur regardless of their effect on the RDF, causes the system to have some small amount of equilibrium-type behavior. This behavior is reflected by the more pronounced extrema in the reconstructed system. However, the actual disk systems themselves are difficult to distinguish visually. Figure 15 shows a realization of the reference RSA systems at $\phi = 0.543$ in (a), and the system which was reconstructed from the initially random system in (b). However, we should point out that we also reconstructed a system with essentially the same RDF, but from an *initially periodic lattice of disks*.

As a quantitative comparison of how the original and reconstructed systems match, we can compare the pore-size distribution $P(r)$ defined in Section 2. This is significantly different information than that contained in $g(r)$, and is therefore a useful way to compare the success of the reconstruction. The pore-size functions are very similar, with the difference

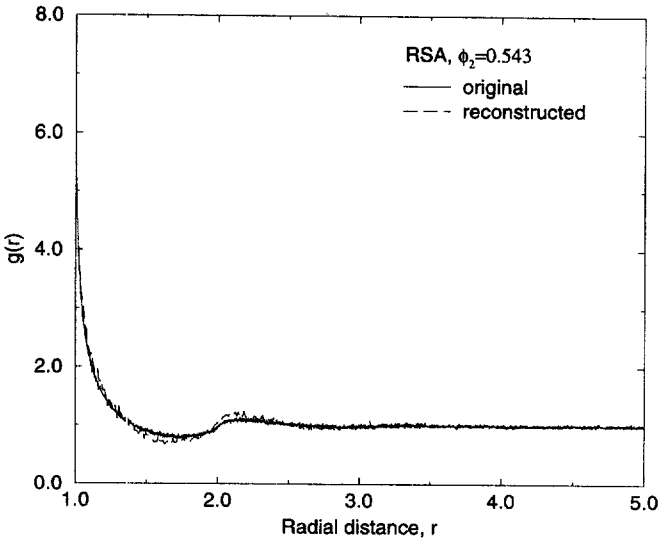

Fig. 14. The radial distribution function (RDF) $g(r)$ vs the dimensionless radial distance r/σ for an RSA system with $\phi = 0.543$ compared to the reconstructed system.

being that the reconstructed system is somewhat longer ranged. This is due to the fact that the reconstructed system tends to "cluster" the particles together in order to get the required contact values, while the original RSA system has very few large pores, due to the nature of the adsorption process. However, this discrepancy is not surprising since there must always be some degree of nonuniqueness.

Our formulation provides a quantitative means by which a system can be reconstructed from one or more correlation functions associated with the original system. This is important because in many experiments, the actual structure of the random many-body system is not known. Rather, it is the structure factor (or equivalently the RDF) that is directly measurable. Our procedure gives one confidence that a reasonable facsimile of the actual structure can be produced from the RDF for a class of many-body systems in which there is not significant clustering of the particles. Elsewhere, we study the reconstruction of many-particle systems that can form clusters (Rintoul and Torquato, 1997) where the use of the RDF is more problematical. However, when clustering is significant one could use correlation functions that reflect connectedness information such as the pair-connectedness function or two-point cluster function.

4.3. *Extensions and other applications*

Although we specialized to equi-sized disks in this simulation, our procedure can treat disks with a size distribution. Moreover, Yeong and Torquato (1998) have recently generalized the procedure to treat digitized images of random media obtained from 2D micrographs or 3D tomographic techniques (Coker *et al.*, 1996). The reconstruction is performed in a manner similar to the disk system by taking an occupied "pixel", and exchanging its position with an unoccupied one. The move is rejected or accepted based on whether or not the new correlation function for the system is "closer" to the reference function. For reconstruction of digitized media, one does not use n-particle distribution functions as the correlation function. Rather we use n-point correlation functions, such as the aforementioned n-point probability function S_n.

Another intriguing inverse problem that we can pursue with this procedure is the construction of heterogeneous media based on the specification of a model or hypothetical statistical correlation function. This question involves understanding the general mathematical properties of realizable correlation functions. Moreover, there are a family of structures that can have the same correlation function. There may be many structures within this family that possess similar effective properties. However, it is likely that some

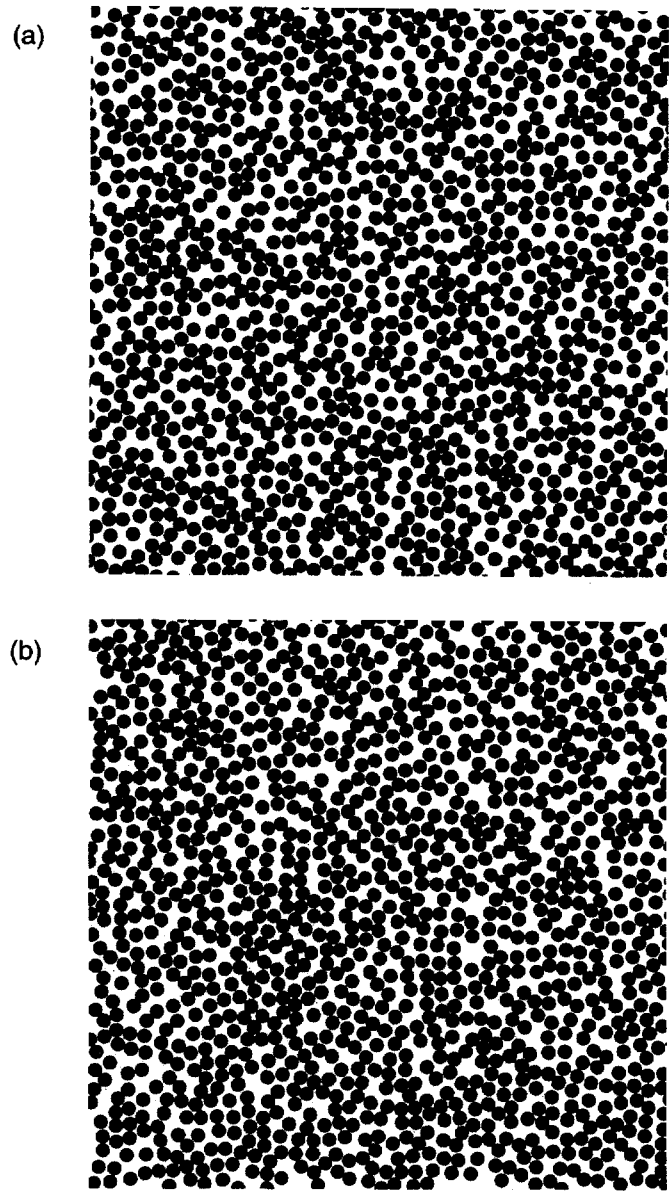

Fig. 15. (a) A portion of a sample RSA system at $\phi = 0.543$; (b) a portion of the reconstructed RSA system at $\phi = 0.543$. The systems are fairly similar, but (b) occasionally contains large void areas which are not seen in the true RSA system.

structures within this family will have markedly different effective properties and it would be of interest to identify the *outliers*. Understanding this question of nonuniqueness as it relates to the effective properties of heterogeneous media will offer great insight into the structure/property relations. This extension will be reported on in a future paper.

Acknowledgements—I am deeply indebted to my collaborators over the last few years (L. Gibiansky, M. Rintoul, J. Quintanilla and C. Yeong) who made invaluable contributions to much of the research described here. I gratefully acknowledge the support of the Office of Basic Energy Sciences of the U.S. Department of Energy under Grant no. DE-FG02-92ER14275 and the Air Force Office of Scientific Research under Grant no. F49620-92-J-0501.

REFERENCES

Abboud, J. H., West, D. R. F. and Rawlings, R. D. (1994) Functionally graded titanium–aluminide composites produced by laser cladding. *Journal of Material Science* **29**, 3393–3398.

Adler, P., Jacquin, C. G. and Quibler, J. A. (1990) Flow in simulated porous media. *International Journal of Multiphase Flow* **16,** 691–712.
Avellaneda, M. and Torquato, S. (1991) Rigorous link between fluid permeability, electrical conductivity, and relaxation times for transport in porous media. *Physics of Fluids A* **3,** 2529–2540.
Barsoum, M. W., Kangutkar, P. and Wang, A. S. D. (1992) Matrix crack initiation in ceramic matrix composite i: Experiments and test results. *Composites Science Technology* **44,** 257–269.
Bear, J. (1972) *Dynamics of Fluids in Porous Media.* Elsevier, New York.
Beran, M. J. (1968) *Statistical Continuum Theories.* Wiley, New York.
Beran, M. J. and Molyneux, J. (1965) Use of classical variational principals to determine bounds for the effective bulk modulus in heterogeneous media. *A. Applied Mathematics* **24,** 107–118.
Berryman, J. G. and Milton, G. W. (1985) Normalization constraint for variational bounds on the fluid permeability. *Journal of Chemistry and Physics* **83,** 754–760.
Berryman, J. G. and Milton, G. W. (1988) Microgeometry of random composites and porous media. *Journal of Physics D: Applied Physics* **21,** 87–94.
Bond, J. R., Kofman, L. and Pogosyan, D. (1996) How filaments of galaxies are woven into the cosmic web. *Nature* **380,** 603–606.
Botsis, J., Beldica, C. and Zhao, D. (1995) On strength scaling of a composite with long aligned fibers. *International Journal of Fracture* **69,** 27–36.
Brooks, S. P. and Morgan, J. T. (1995) Optimization using simulated annealing. *The Statistician* **82,** 241–257.
Bruno, O. (1991) Effective conductivity of strongly heterogeneous composites. *Proceedings of the Royal Society of London A* **433,** 353–381.
Cherradi, N., Kawasaki, A. and Gasik, M. (1994) Worldwide trends in functional gradient materials research and development. *Composites Engineering* **4,** 883–894.
Chiew, Y. C., Glandt, E. D. and Stell, G. (1985) Clustering and percolation in multicomponent systems of randomly centered and permeable spheres. *Journal of Chemistry and Physics* **83,** 761–772.
Christensen, R. M. (1979) *Mechanics of Composite Materials.* Wiley, New York.
Chung, I. and Weitsman, Y. (1994) A mechanics model for the compressive response of fiber reinforced composites. *International Journal of Solids and Structures*, 2519–2536.
Coker, D., Torquato, S. and Dunsmuir, J. (1996) Morphological and physical properties of fontainebleu sandstone from tomographic analysis. *Journal of Geophysical Research* **100,** 17497–17506.
Coniglio, A., DeAngelis, U. and Forlani, A. (1977) Pair connectedness and cluster size. *Journal of Physics A* **10,** 1123–1139.
Doi, M. (1976) A new variational approach to the diffusion and flow problem in porous media. *Journal of the Physics Society of Japan* **40,** 567–572.
Duxbury, P. M. and Leath, P. L. (1994) Failure probability and average strength of disordered systems. *Physics Review Letters* **72,** 2805–2808.
Eischen, J. and Torquato, S. (1993) Determining elastic behavior of composites by the boundary element method. *Journal of Applied Physics* **74,** 159–170.
Feder, J. (1980) Random sequential adsorption. *Journal of Theoretical Biology* **87,** 237–254.
Fukui, Y., Takashima, K. and Ponton, C. B. (1994) Measurement of Young's modulus and internal friction of an *in situ* Al–Al_3Ni functionally graded material. *Journal of Material Science* **29,** 2281–2288.
Gelhar, L. W. (1993) *Stochastic Subsurface Hydrology.* Prentice-Hall, Englewood Cliffs, New Jersey.
Gibiansky, L. and Torquato, S. (1993) Link between the conductivity and elastic moduli of composite materials. *Physics Review Letters* **71,** 2927–2930.
Gibiansky, L. and Torquato, S. (1995) Rigorous link between the conductivity and elastic moduli of fiber-reinforced composite materials. *Philosophical Transactions of the Royal Society of London* **343,** 243–278.
Gibiansky, L. and Torquato, S. (1996a) Bounds on the effective moduli of cracked materials. *Journal of Mechanics and Physics of Solids* **44,** 233–242.
Gibiansky, L. and Torquato, S. (1996b) Connection between the conductivity and elastic moduli of isotropic composite materials. *Proceedings of the Royal Society of London A* **452,** 253–283.
Hansen, J. P. and McDonald, I. R. (1986) *Theory of Simple Liquids.* Academic Press, New York.
Hashin, Z. (1983) Analysis of composite materials. *Journal of Applied Mechanics* **50,** 481–505.
Hashin, Z. and Shtrikman, S. (1962) A variational approach to the theory of the effective magnetic permeability of multiphase materials. *Journal of Applied Physics* **33,** 3125–3131.
Hashin, Z. and Shtrikman, S. (1963) A variational approach to the elastic behavior of multiphase materials. *Journal of the Mechanics and Physics of Solids* **4,** 286–295.
Haubensack, F. G., Bulatov, V. V and Argon, A. S. (1995) Simulation of crack propagation resistance in brittle media of high porosity. *Computer-Aided Material and Design* **2,** 205–230.
Kim, I. and Torquato, S. (1990) Determination of the effective conductivity of heterogeneous media by Brownian motion simulation. *Journal of Applied Physics* **68,** 3892–3903.
Lado, F. and Torquato, S. (1990) Two-point probability function for distributions of oriented hard ellipsoids. *Journal of Chemistry and Physics* **93,** 5912–5917.
Lu, B. and Torquato, S. (1990a) Local volume fraction fluctuations in heterogeneous media. *Journal of Chemistry and Physics* **93,** 3452–3459.
Lu, B. and Torquato, S. (1990b) *n*-point probability functions for a lattice model of heterogeneous media. *Physical Review B* **42,** 4453–4459.
Lu, B. and Torquato, S. (1991) General formalism to characterize the microstructure of polydispersed random media. *Physical Review A* **43,** 2078–2080.
MacKay (1990) Effect of fiber spacing on interfacial damage in a metal matrix composite. *Scripta Metallica* **24,** 167–172.
McCoy, J. J. (1970) *Recent Advances in Engineering Sciences.* Gordon and Breach, New York.
Milton, G. W. (1982) Bounds on the elastic and transport properties of two-component composites. *Journal of Mechanics and Solids* **30,** 177–191.
Milton, G. W. (1984) *Physics and Chemistry of Porous Media.* American Institute of Physics.

Milton, G. W. and Phan-Thien, N. (1982) New bounds on the effective moduli of two-component materials. *Proceedings of the Royal Society of London A* **380,** 305–331.
Nadeau, J. C. and Ferrari, M. (1995) Second-rank equilibrium and transport properties of fibrous composites: effective predictions and bounds. *Composites Engineering* **5,** 821–838.
Ostoja-Starzewski, M. (1994) Micromechanics as a basis of continuum random fields. *Applied Mechanics Review* **47,** S221–S230.
Ostoja-Starzewski, M., Sheng, P. and Jasiuk, I. (1994) Influence of random geometry on effective properties and damage formation in 2-d composites. *ASME Journal of Engineering Material Technology* **116,** 384–391.
Perrins, W. T., McKenzie, D. R. and McPhedran, R. C. (1979) Transport properties of regular arrays of cylinders. *Proceedings of the Royal Society of London A* **369,** 207–214.
Prager, S. (1963) Diffusion and viscous flow in concentrated suspensions. *Physica* **29,** 129–139.
Quintanilla, J. and Torquato, S. (1997a) Local volume fraction fluctuations in random media. *Journal of Chemistry and Physics* **106,** 2741–2751.
Quintanilla, J. and Torquato, S. (1997b) Microstructure functions for a model of statistically inhomogeneous random media. *Physics Review E* **55,** 1558–1565.
Reiter, T., Dvorak, G. J. and Tvergaard, V. (1997) Micromechanical models for graded composite materials. *Journal of Mechanics and Physics of Solids* **45,** 1281–1302.
Rintoul, M. and Torquato, S. (1997) Reconstruction of the structure of dispersions. *Journal of Colloid Interface Science* **186,** 467–476.
Royden, H. (1988) *Real Analysis*, 3rd edn. Macmillan, New York.
Rubinstein, J. and Torquato, S. (1988) Diffusion-controlled reactions: mathematical formulation, variational principles, and rigorous bounds. *Journal of Chemistry and Physics* **88,** 6372–6380.
Rubinstein, J. and Torquato, S. (1989) Flow in random porous media: mathematical formulation, variational principles and rigorous bounds. *Journal of Fluid Mechanics* **206,** 25–46.
Sanchez-Palencia, E. (1980) Nonhomogeneous media and vibration theory. Lecture notes in physics. Springer, Berlin.
Silnutzer, N. (1972) Effective constants of statistically homogeneous materials. Ph.D. thesis, University of Pennsylvania, Philadelphia.
Stell, G. (1984) Exact question for the pair-connectedness function. *Journal of Physics A* **17,** L855–L858.
Stoyan, D., Kendall, W. S. and Mecke, J. (1995) *Stochastic Geometry and Its Applications*, 2nd edn. Wiley, New York.
Torquato, S. (1986a) Bulk properties of two-phase disordered media, iii: new bounds on the effective conductivity of dispersions of penetrable spheres. *Journal of Chemistry and Physics* **84,** 6345–6359.
Torquato, S. (1986b) Microstructure characterization and bulk properties of disordered two-phase media. *Journal of Statistic Physics* **45,** 843–873.
Torquato, S. (1990) Relationship between permeability and diffusion-controlled trapping constant of porous media. *Physics Review Letters* **64,** 2644–2647.
Torquato, S. (1991) Random heterogeneous media: microstructure and improved bounds on the effective properties. *Applied Mechanics Review* **44,** 37–76.
Torquato, S. (1992) Connection between the morphology and effective properties of heterogeneous materials macroscopic behavior of heterogeneous materials from the microstructure. (eds) S. Torquato and D. Krajcinovic. Vol. 147,*American Society of Mechanical Engineers AMD* pp. 53–65.
Torquato, S. (1995) Mean nearest-neighbor distance in random packings of d-dimensional hard spheres. *Physics Review Letters* **74,** 2156–2159.
Torquato, S. (1997) Effective stiffness tensor of composite media: I. Exact series expansions. *Journal of Mechanics and Physics of Solids* **45,** 1421–1448.
Torquato, S. and Avellaneda, M. (1991) Diffusion and reaction in heterogeneous media: pore size distribution, relaxation times, and mean survival time. *Journal of Chemistry and Physics* **95,** 6477–6489.
Torquato, S. and Kim, I. (1992) Cross-property relations for momentum and diffusional transport in porous media. *Journal of Applied Physics* **72,** 2612–2619.
Torquato, S. and Lado, F. (1992) Improved bounds on the effective elastic mod of random arrays of cylinders. *Journal of Applied Mechanics* **59,** 1–6.
Torquato, S. and Lu, B. (1993) Chord-length distribution function for two-phase random media. *Physics Review E* **47,** 2950–2953.
Torquato, S. and Rintoul, M. (1995) Effect of the interface on the properties of composite media. *Physics Review Letters* **75,** 4067–4070.
Torquato, S. and Rubinstein, J. (1991) Improved bounds on the effective conductivity of high contrast suspensions. *Journal of Applied Physics* **69,** 7118–7125.
Torquato, S. and Sen, A. (1990) Conductivity tensor of anisotropic composite media from the microstructure. *Journal of Applied Physics* **67,** 1145–1155.
Torquato, S. and Stell, G. (1985) Microstructure of two-phase random media. V. The *n*-point matrix probability functions for impenetrable spheres. *Journal of Chemistry and Physics* **82,** 980–987.
Torquato, S., Beasley, J. and Chiew, Y. (1988) Two-point cluster function for continuum percolation. *Journal of Chemistry and Physics* **88,** 6540–6546.
Widom, W. (1966) Random sequential addition of hard spheres to a volume. *Journal of Chemistry and Physics* **44,** 3888–3894.
Willis, J. R. (1981) Variational and related methods for the overall properties of composite. In *Advances in Applied Mechanics*, Vol. 21. Academic Press, New York.
Yeong, C. L. Y. and Torquato, S. (1998) Reconstructing random media. *Physical Review E* **57,** 495–506.
Zhou, S. J. and Curtin, W. A. (1995) Failure of fiber composites: a lattice green function approach. *Acta Metallica Materiala* **43,** 3093–3104.
Zuiker, J. and Dvorak, G. J. (1994) The effective properties of functionally graded composites: I. Extension of the Mori-Tanaka method to linearly varying fields. *Composites Engineering* **4,** 19–35.